Asian Journal of Chemistry; Vol. 38, No. 6 (2026), 1547-1555
ASIAN JOURNAL OF CHEMISTRY
https://doi.org/10.14233/ajchem.2026.35772

Effect of 1,1-Diamino-2,2-Dinitroethene (FOX-7) on Thermal Decomposition of Cyclotetramethylenetetranitramine (HMX) and Combustion of Reduced Smoke Propellants

S.S.N.M. SANTOSH MADA[1,*], VAIBHAV S. SADAVARTE[1], RAMESH KURVA[1], SHRIKANT M. PANDE[1] and PRASHANT S. KULKARNI[2]

[1]High Energy Materials Research Laboratory, Pune-411021, India
[2]Defence Institute of Advanced Technology, Pune-411025, India

*Corresponding author: E-mail: santosh.mada.hemrl@gov.in

Received: 17 February 2026 *Accepted*: 2 May 2026 *Published online*: 31 May 2026 AJC-22381

The development of next generation solid rocket propellant requires a critical balance between high energy output and insensitivity to mechanical stimuli. This study investigates the thermal decomposition of cyclotetramethylenetetranitramine (HMX) in combination with 1,1-diamino-2,2-dinitroethene (FOX-7) and other propellant ingredients. Mixture of FOX-7 and HMX was analysed by SEM and XRD techniques to understand the type of interactions formed during sample preparation by wet grinding process. Further, thermogravimetric analysis coupled with FTIR (TG-FTIR) was employed to investigate the thermal decomposition behaviour of HMX/FOX-7 binary mixtures and solid propellant formulations containing butanetriol trinitrate, polycaprolactone polyol prepolymer, HMX, FOX-7 and ammonium perchlorate (AP). In this study, neat HMX exhibited a single sharp exothermic peak at 285.7 ºC, whereas FOX-7 decomposed in two stages at 230.5 and 293.9 ºC. Decompositions occurred at 225.2 ºC, 254.1 ºC and 285.0 ºC in 1:1 HMX/FOX-7 mixture, indicating significant mutual interaction between the two components. Similar type of interaction was also observed in thermal decomposition of FOX-7/AP combination. In addition, a systematic study of binary mixtures was conducted to understand the mutual effect of FOX-7 on thermal decomposition of HMX. An attempt to predict the mechanism of mutual effect of FOX-7 and HMX on thermal decomposition of 1:1 mixture has also been made by FTIR absorbance intensity of gases evolved at maximum heat release. Propellants designated as P-1, P-2 and P-3 were formulated using unary, binary and ternary solid mixtures of FOX-7, HMX and AP, respectively, and were characterized for density, sensitivity and thermal stability. It was observed that pressure dependencies of P-2 and P-3 were reduced by ~6% and ~11%, respectively as a result of the mutual effect among the propellant ingredients.

Keywords: Mutual effect, Thermal decomposition, Pressure exponent, FTIR absorbance intensity.

INTRODUCTION

Cyclotetramethylenetetranitramine (HMX) based advanced energetic propellants are always the best choice for reduced smoke applications due to its high thermal stability, high density, energy and smokeless features. Nitramine propellants containing HMX deliver higher specific impulses due to lower molecular weight combustion gases even though adiabatic flame temperatures are relatively low [1]. Despite the attractive features of HMX, nitramine propellants have some drawbacks in terms of ballistic properties such as higher pressure exponent (> 0.6) and insensitiveness towards burn rate catalysts [2-4]. Burning rates of non-ammonium perchlorate based formulations having high HMX content are independent of the variation of particle size of HMX in contrast to ammonium perchlorate (AP) based formulations, wherein strong dependence of burning rate on the surface area of AP exists [5]. Also, nitramine based formulations are having higher sensitivity to mechanical stimuli which leads to accidental initiation of rockets, munitions and explosive charges [6].

In defense technology, high performance propulsion systems are fuelled with reduced smoke propellants [4,7-12] and they exhibit reduced exhaust signature for the intended stealth purpose due to the absence of primary smoke in plume. In these, oxidizers such as HMX, AP, ammonium nitrate (AN), 1,3,5-trinitro-1,3,5-triazine (RDX), ammonium dinitramide (ADN), *etc.* are used and the metal powders are avoided to make the propellant free of primary smoke. However, AP and HMX duo outperform the other combinations for reduced smoke applications in terms of energy and density. Higher

content of HMX leads to uncontrolled ballistic parameters and higher AP causes high occurrence of secondary smoke in the exhaust. Therefore, there is always constant quest to replace fully or partially AP and HMX in the propellant formulation without compromising of performance parameters.

1,1-diamino-2,2-dinitroethene (FOX-7) is an insensitive high explosive that has attracted considerable attention due to its high density and high thermal stability [13-17]. These attributes make it an ideal candidate for use in advanced energetic propellants and insensitive munitions, particularly as a potential co-component with more sensitive propellant formulations such as HMX based advanced energetic propellants. The thermal interaction between FOX-7 and HMX is not fully understood, despite their generally favourable compatibility in propellant formulations. The examination of this interaction whether FOX-7 acts synergistically, suppressively or catalytically in propellant formulation with HMX has not been fully resolved [18]. Understanding these interactions is very important for the development of next generation and low sensitive advanced propellant formulations.

In this work, an attempt has been made to investigate the mutual effect of FOX-7 on thermal decomposition behaviour of HMX and AP through DSC, TGA and TG-FTIR. Mutual interaction refers to the simultaneous and bidirectional influence of two or more molecules on each other during the thermal decomposition process. The present work focuses on investigating variations in decomposition behaviour, heat release and evolved gaseous species by comparing individual components, their physical mixtures and formulated propellants under controlled conditions. In addition, possible mutual interactions occurring during thermal decomposition were examined. These insights into thermal interactions may contribute to the rational design of next-generation energetic propellant formulations with improved safety and performance.

EXPERIMENTAL

The chemicals *viz*., ammonium perchlorate (Pandian Chemicals, India, >99%, 50 μm), FOX-7 (make: Inhouse, >99%, 15 μm) and HMX (Solar Industries, Nagpur, India, >99%, particle sizes: 9 μm and 135 μm) were used. Polyurethane energetic binder consisting of butanetrioltrinitrate (Bharat Explosives Ltd., India, >99%), polycaprolactone polyol (make: Inhouse, m.w.: ~6500), 2-nitrodiphenylamine (Speciality Products Research Group, Pune, India, > 97%) and isophorone diisocyanate (TCI, Japan, > 99%) was used as binder system for propellant formulations.

Wet grinding method was preferred over the available techniques to prepare the physical mixture of solids. The possible interaction between the solids are hydrogen bonding and weak van der Waal's force of attraction, due to which physical interaction may exist and agglomeration may occur on HMX surface after drying. It enables safe particle size reduction in a liquid medium and facilitates close proximity between the particles. Binary mixtures of FOX-7 & HMX, FOX-7 & AP and ternary mixture of FOX-7, AP & HMX in various weight ratios have been prepared using ceramic mortar and pestle by wet grinding technique with water as medium. Mixture was dried for 48 h at 323 K and 72 h in desiccator.

Characterization: Thermogravimetric analysis (TGA) was performed using a TGA 8000 (Perkin-Elmer, USA) coupled with FT-IR under a nitrogen atmosphere. Surface morphology was examined using an environmental scanning electron microscope (ESEM, Quanta 200, FEI Company, USA). X-ray diffraction (XRD) patterns were recorded using a Bruker D8 Advance diffractometer (Bruker AXS, Germany) with Cu*K*α radiation (λ = 1.5406 Å). Impact sensitivity was determined using a BAM fall hammer apparatus (*e.g.* BAM Fallhammer, OZM Research/ERL, Germany), where a defined mass is dropped from variable heights onto the sample to determine the characteristic drop height (H_{50}).

Propellant sample preparation and testing: Propellant ingredients were mixed using a 5 L vertical mixing system. The formulations consisted of 75% solid loading and 25% polyurethane-based energetic binder system containing unary, binary and ternary combinations of FOX-7, HMX and AP. Propellant mix was cast under vacuum and cured at 333 K for 144 h. Propellant samples were cut to 6 mm × 6 mm × 130 mm strands. Propellant burning rates were determined in modified crawford bomb under nitrogen atmosphere at 4.9, 6.9 and 8.8 MPa using acoustic emission technique.

RESULTS AND DISCUSSION

Morphology and structural studies: The β-HMX sample predominantly exhibits well defined geometrical crystal morphology as shown in Fig. 1a, whereas both FOX-7 and FOX-7/β-HMX mixture display irregular and non-geometric morphology in Fig. 1b and Fig. 1c-f, respectively. This morphological feature suggests possible presence of amorphous or poor crystalline regions within FOX-7 and FOX-7/β-HMX mixture. The observed particle size reduction of mixture during wet grinding can be attributed to mechanical shear and impact forces, which lead to the fracture of FOX-7 and β-HMX crystals. This may generate fresh surfaces with higher surface energy, thereby promoting the agglomeration, resulting in heterogenous clusters and localised surface coverage rather than uniform coating. This accumulation of agglomerated particulates of FOX-7 on β-HMX may reduce direct exposure of β-HMX crystals to any stimuli, potentially contributing towards the thermal decomposition behaviour. The mean particle size measured for the FOX-7/β-HMX mixture was X_{mean} = 60.65 μm. Primary observations from the micrographs of mixture reveal that the interaction between the FOX-7 and β-HMX crystals is purely physical.

These observations support that the FOX-7/β-HMX mixture (mass ratio 1:1) retains the structural identity of individual components, which may influence the thermal decomposition behaviour of the mixture.

Powder XRD studies: The XRD spectra (Fig. 2) shows the crystallographic profiles of virgin HMX and virgin FOX-7 and their combined mixture over a 2θ range of 10º and 50º. The virgin HMX sample exhibits a well-defined, highly crystalline structure characterised by sharp, prominent diffraction peaks at 14.7º, 16.0º, 20.5º, 27.2º and a distinct maximum at 31.9º. In contrast, neat FOX-7 diffractogram represents a different crystallographic signature, dominated by an intense primary reflection at 27.8º and 26.7º, along with minor peaks

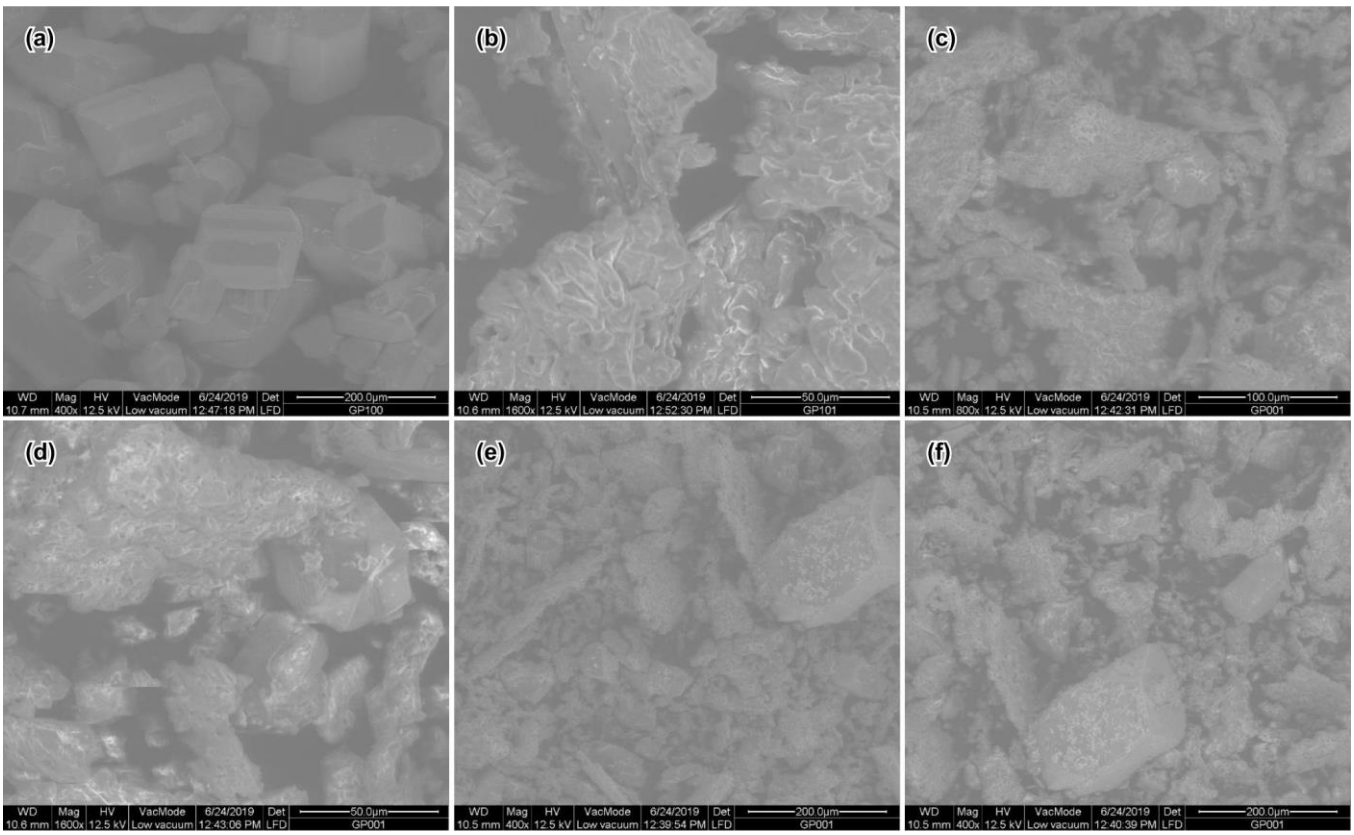

Fig. 1. SEM micrographs (a) β-HMX, (b) FOX-7 and (c-f) of FOX-7/β-HMX mixture (mass ratio 1:1)

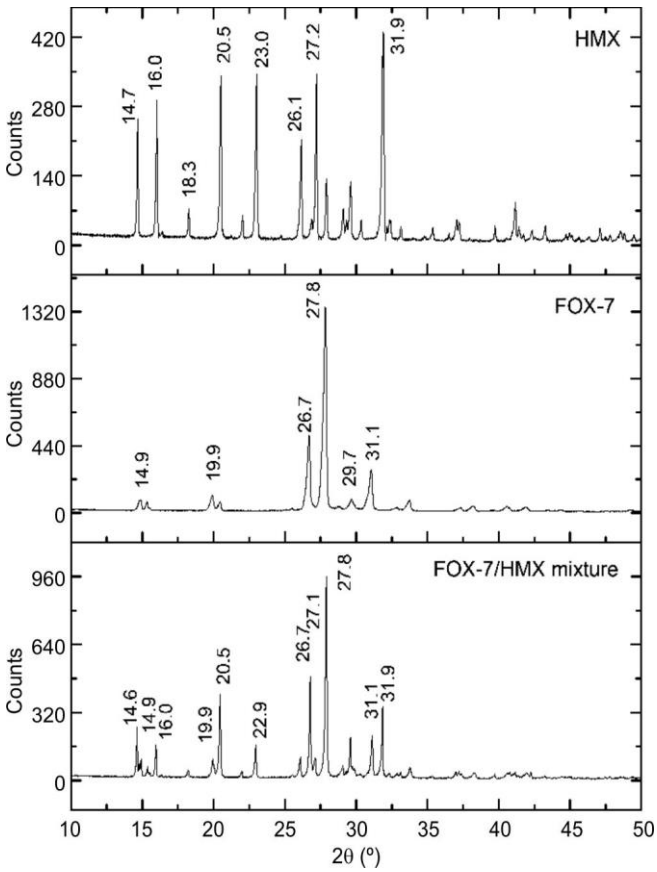

Fig. 2. Comparative PXRD patterns of HMX, FOX-7 and FOX-7/HMX mixture

at 14.9º, 19.9º and 31.1º. These individual diffractograms serve as excellent reference baselines, clearly establishing the unique spatial arrangements and lattice planes inherent to each energetic material.

An analysis of the FOX-7/HMX mixture reveals that the resulting diffractogram is essentially a direct superposition of the two individual starting materials, indicating a simple physical mixture rather than a new crystallographic phase. The characteristic key peaks from both components are clearly preserved and identifiable in the mixture without significant angular shifting; for example, the HMX markers are at 16.0º, 20.5º and 31.9º appear alongside the defining FOX-7 markers at 19.9º, 26.7º and 27.8º. The absence of any new diffraction peaks, combined with the lack of significant peak shifting, suggests that no co-crystallisation or structural integration has occurred between the HMX and FOX-7 domains in this specific formulation.

Thermal studies: TGA and DSC curves of FOX-7, β-HMX and FOX-7/β-HMX (mass ratio 1:1) at heating rate 10 ºC/min are shown in Figs. 3 and 4, respectively. In DSC, FOX-7 has exhibited two endothermic peaks, one is at 116.8 ºC for α→β and other is 178.7 ºC for β→γ phase changes. Kempa *et al.* [19] have studied phase transitions of FOX-7 by XRD measurements and observed α→β transition at 116 ºC and β→γ at 173 ºC. Several reports [20,21] showed these transitions occurred in the range of 113 ºC to 116 ºC for α→β and around 173 ºC for β→γ. The difference in the peak temperatures of these transitions may be attributed to the purity and physical state of the materials such as uncrystallised and recrystallised forms.

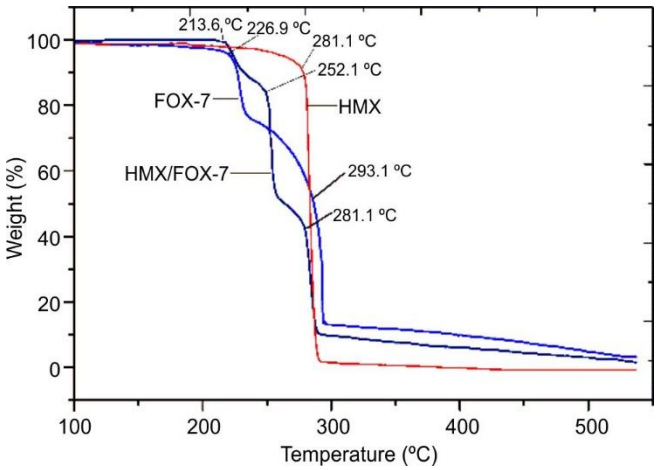

Fig. 3. Thermograms of HMX, FOX-7 and HMX/FOX-7 (1:1) decompositions with onset decomposition temperatures

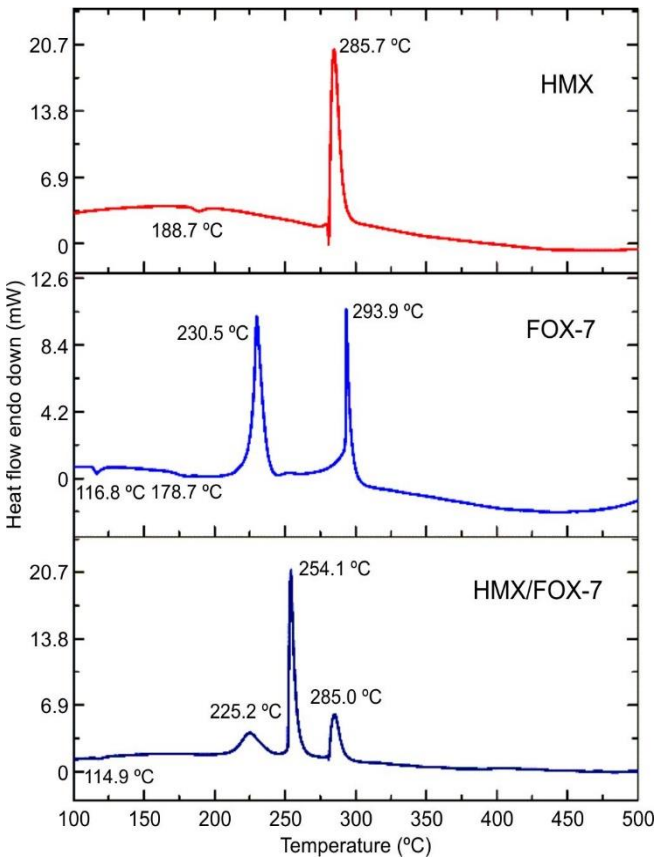

Fig. 4. DSC curves of HMX, FOX-7 and HMX/FOX-7 (1:1) decompositions with peak decomposition temperatures

Above 200 ºC, two exothermic peaks were observed for FOX-7 decomposition without melting. These decompositions were ascribed to two phases, *i.e.* crystalline and amorphous phases of FOX-7 and occurred at peak temperatures 230.5 ºC and 293.9 ºC, respectively [22,23]. A two-stage mass loss corresponding to the exothermic peaks in the DSC curve was observed in the TG analysis. The first decomposition stage started at 227 ºC and accounted for a 24% weight loss, whereas the second stage commenced at 293 ºC with a weight loss of 62%. The results are comparable with the literature [17].

According to Figs. 3 and 4, HMX exhibited an endothermic event at 188.7 ºC attributed to the β→δ crystal phase transition. A weak endothermic peak related to melting was further observed at 280.0 ºC in the DSC curve. Subsequently, HMX decomposed exothermically with a peak temperature of 285.7 ºC and significant energy evolution. TGA analysis demonstrated a single-step decomposition process with approximately 97% mass loss and an onset decomposition temperature of 281.1 °C. These thermal characteristics are in good correlation with published reports [24].

Thermal stability of β-HMX in the presence of FOX-7 and the effect of FOX-7 on the decomposition of β-HMX has been studied with the help of TGA and DSC of FOX-7/β-HMX (1:1) mixture. From Figs. 3 and 4, FOX-7/β-HMX mixture decomposed in three stages in contrast to the neat solids *i.e.* β-HMX and FOX-7. In TGA, the peak temperature of first exothermic decomposition decreased from 230.5 ºC to 225.2 ºC with a weight loss of approximately 14.5%. Second exothermic decomposition of the mixture was observed at 254.1 ºC with weight loss of 38.5%, which is not observed during either FOX-7 or β-HMX decomposition. Similar observations were also recorded in the DSC thermogram.

Thermal analysis of FOX-7/HMX (4:1) co-crystals by Ghosh *et al*. [18] reported that first exothermic decomposition peak shifted to 247 ºC and second exothermic decomposition peak combined with HMX decomposition, at 278 ºC. Due to the incorporation of β-HMX and FOX-7 in the same crystalline structure, decompositions are more influenced compared to physical mixture of the present study.

Non-isothermal decomposition kinetics: The kinetic parameters for decomposition of the FOX-7, β-HMX and FOX-7/β-HMX mixture (1:1 mass ratio) were ascertained from the results of DSC analysis conducted at multiple heating rates using non-isothermal kinetic methods such as Kissinger the mathematical representation of Kissinger and Ozawa models [25-27] are given as follows:

Kissinger equation:

$$\ln\left(\frac{\beta}{T^2}\right) = \ln\left(\frac{RA}{E}\right) - \frac{E}{RT}$$

Ozawa equation:

$$\ln\beta = -\frac{E}{RT} + \ln\left(\frac{RA}{E}\right) + \text{Constant}$$

where β is linear heating rate (K/min), R is the universal gas constant: 8.314 J K^{-1} mol^{-1}, A is pre-exponential or frequency factor, E is activation energy and T is peak decomposition temperature.

These models are based on the fact that increasing the heating rate gives less time to react at lower temperature and hence, decomposition is delayed. As a result, the maximum reaction temperature shifts to higher side with increasing heating rate. In this study, DSC thermograms were recorded at four different heating rates 5 ºC/min, 10 ºC/min,15 ºC/min and 20 ºC/min. The activation energies (E_a) are calculated used using Kissinger and Ozawa methods and presented in Table-1.

Activation energy of maximum heat release decomposition of mixture has been found to be significantly higher

TABLE-1
EXPERIMENTAL KINETIC PARAMETERS OF FOX-7, HMX AND FOX-7/β-HMX (1:1 MASS RATIO) OF MAXIMUM HEAT RELEASING PEAKS

Material	B (ºC/min)	T_{max} (ºC)	E_a (kcal/mol)	
			Kissinger	Ozawa
FOX-7	5	286.4	58.98	58.20
	10	293.9		
	15	297.0		
	20	301.2		
HMX	5	282.0	102.74	99.81
	10	285.7		
	15	288.8		
	20	289.9		
FOX-7/ HMX mixture	5	251.8	123.02	118.94
	10	254.1		
	15	256.2		
	20	257.9		

compared to virgin FOX-7 with the value E_a = 123.02 kcal/mol, indicating an enhancement of thermal stability. This may be due to the intermolecular interaction enhancement and hydrogen bonding between the -NH_2 groups of FOX-7 and NO_2 groups of HMX. This induces reduced reactivity and improved thermal resistance. The obtained results are in line with the reported values [18,28].

Mechanistic studies of thermal decomposition by FTIR: FTIR spectra of the gaseous products evolved during FOX-7 decomposition are shown in Fig. 5, recorded at the point of maximum FTIR intensity corresponding to a temperature of approximately 230.1 ºC. As illustrated in Fig. 5, the decomposition products identified in the FTIR spectra include H_2O, CO_2, N_2O, NO_2, nitric acid and nitrile oxide intermediates. These observations are in close agreement with previously reported literature findings [14]. These products are formed by initial C-NO_2 bond cleavage and intramolecular proton transfer resulting to the elimination of HNO_2 from the FOX-7 molecule. Minor quantity of NO_2 is observed in this stage. The temperature of second stage decomposition of FOX-7 is 293.9 ºC. Initial decomposition of FOX-7 develops an environment with oxidizing species which promotes the further decomposition. Decomposition products in the second stage is almost similar to first stage and absorbance intensity of NO_2 is higher in contrast to first stage.

The FTIR spectra (Fig. 5) reveal the evolution of N_2O and HCN during the decomposition of neat HMX at 285 ºC. In the HMX/FOX-7 system, decomposition was promoted by NO_2 released from FOX-7. Mixing FOX-7 with HMX in an equimolar proportion resulted in NO_2-induced decomposition at 254.1 ºC owing to homolytic cleavage of the N–N bond. The generation of N_2O through recombination reactions involving NO_2 and NO_x species indicates C–N bond rupture within HMX molecules, thereby validating HMX decomposition at this temperature [29]. This mechanism is commonly associated with nitramine decomposition and is reflected by the intense N_2O peaks observed at 254.1 ºC and 285 ºC for the mixture.

Thermal decomposition of FOX-7/β-HMX mixture (mutual interaction): It is evident from Figs. 3 and 4, that some mutual interaction exists on both materials due to the presence of FOX-7 and HMX simultaneously. To examine the

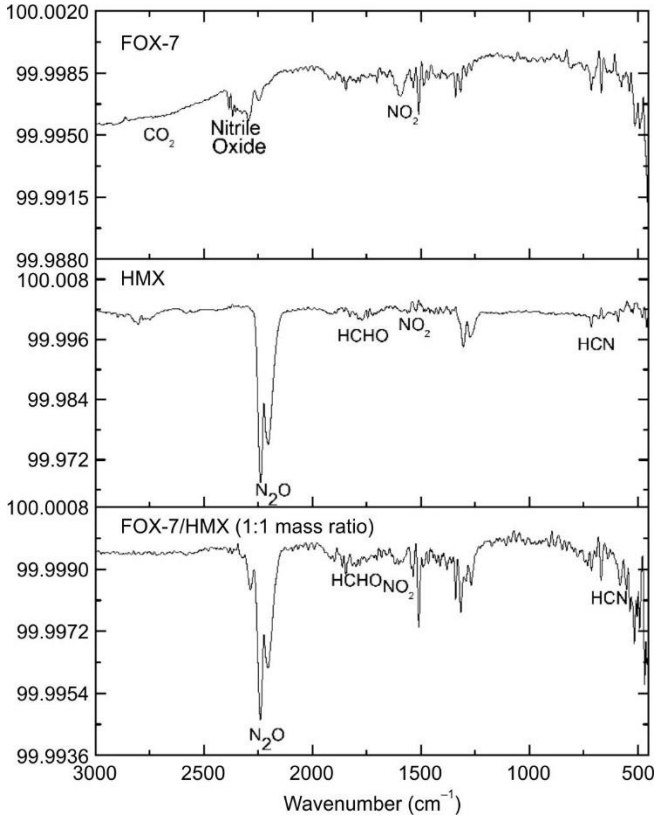

Fig. 5. FTIR spectra of FOX-7, β-HMX and FOX-7/β-HMX mixture (mass ratio 1:1) decomposition products at heating rate of 10 ºC/min at the maximum DSC signal

mutual interaction of FOX-7 and HMX during thermal decomposition, detailed investigations were performed using coupled analytical techniques such as TG-FTIR.

The thermal decomposition mechanism is characterised by the evolution of NO_2 and N_2O, predominantly correspond to the decomposition of FOX-7 and HMX, respectively. Similar decomposition behaviour of nitramines has also been reported [30,31]. Therefore, the FTIR absorbance intensities of these gaseous products were used to identify the onset and peak decomposition stages. Although a minor amount of N_2O was observed during FOX-7 decomposition, it did not interfere with the qualitative interpretation of the TG-FTIR spectra.

FTIR absorbance intensities of NO_2 (1598 cm^{-1}) and N_2O (2238 cm^{-1}) *vs.* temperature were plotted for HMX, FOX-7 and FOX-7/HMX mixture. Higher NO_2 FTIR absorbance intensity (1598 cm^{-1}) was observed at 293.9 ºC in case of neat FOX-7 decomposition and which is evolving with the second stage decomposition of FOX-7. The characteristic wavenumber of N_2O *i.e.* 2238 cm^{-1} was evolved during neat HMX decomposition and it is maximum at the decomposition temperature ~285 ºC (Fig. 6).

In the HMX:FOX-7 mixture, the maximum NO_2 absorbance intensity was observed only at 254.1 ºC, unlike pristine FOX-7 which showed a second-stage decomposition peak at 293.9 ºC. This indicates that the decomposition behaviour of FOX-7 was significantly influenced by the presence of HMX, resulting in the complete shift of the second-stage decomposition from 293.9 ºC to 254.1 ºC. The maximum N_2O absorbance intensities observed at 254.1 ºC and 285.0 ºC (Fig. 6)

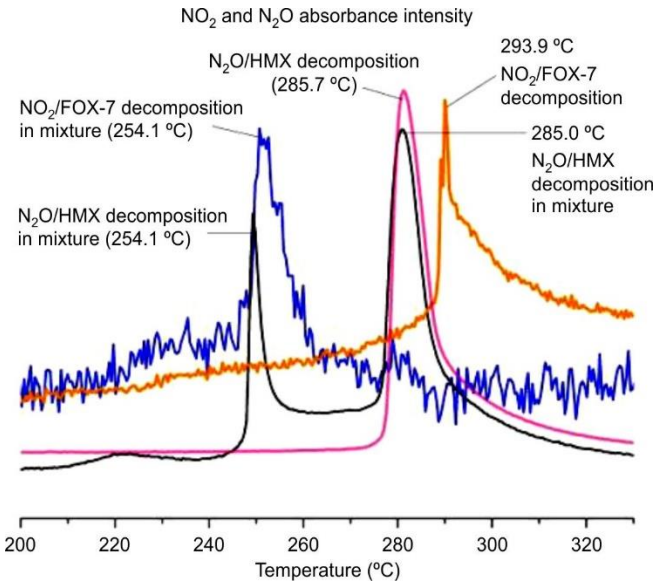

Fig. 6. FTIR absorbance intensities of NO_2 (1598 cm^{-1}) and N_2O (2238 cm^{-1}) of HMX, FOX-7 and HMX/FOX-7 (1:1) *vs.* temperatures (not as per scale)

suggest that unlike neat HMX, the 1:1 HMX/FOX-7 mixture undergoes decomposition in two stages. Therefore, the thermal decomposition behaviour of HMX was also altered in the presence of FOX-7. Similarly, the decomposition peaks of FOX-7 shifted from 230.1 ºC and 293.9 ºC to 225.2 ºC and 254.1 ºC, respectively, confirming mutual interaction between the two energetic materials during decomposition.

To further investigate the effect of FOX-7 concentration on HMX decomposition, HMX/FOX-7 mixtures with ratios of 1:2 and 2:1 were examined. In both mixtures, HMX decomposition occurred at 254.1 ºC and 285.0 ºC, similar to the 1:1 mixture, while the peak area at 254.1 ºC increased proportionally with FOX-7 content. In the 2:1 mixture, the decomposition peak at 285.0 ºC became significantly weaker, indicating a strong influence of FOX-7 on HMX decomposition. These observations confirm the existence of mutual interactions during the thermal decomposition of HMX/FOX-7 mixtures.

Further studies covering compositions from 1:10 to 10:1 revealed that the exothermic decomposition behaviour strongly depends on the HMX/FOX-7 ratio (Fig. 7). Neat HMX and FOX-7 decomposed at approximately 285 ºC and 230 ºC, respectively, with heat release proportional to their content in the mixture. Above 40% HMX content, a prominent exothermic peak corresponding to HMX decomposition at 285 ºC was observed. However, below 30% HMX content, the characteristic HMX decomposition peak at 285 ºC disappeared and the second-stage decomposition peak of FOX-7 at 293.9 ºC was absent in all binary mixtures.

These results indicate that FOX-7 decomposition is strongly dependent on the presence of HMX across the entire composition range, with decomposition shifting predominantly to 254.1 ºC. The heat release at 254.1 ºC increased with FOX-7 content up to 50%, reached a maximum at the equimolar composition and subsequently decreased at higher FOX-7 concentrations. Thus, the mutual influence of FOX-7 and HMX on thermal decomposition is evident in all binary mixtures and strongly depends on the composition ratio.

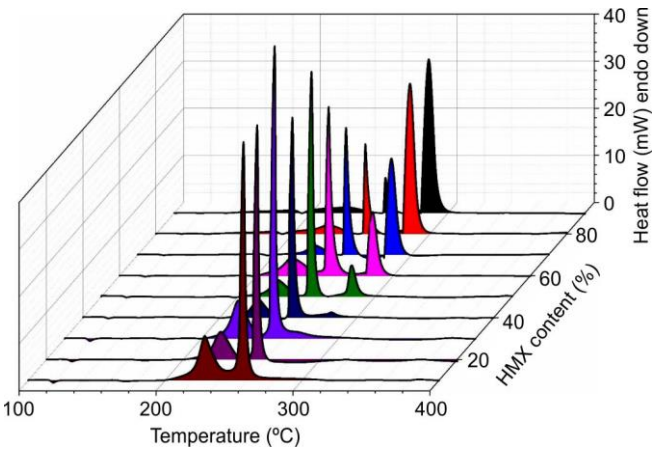

Fig. 7. DSC curves of HMX/FOX-7 mixtures as a function of HMX content

Effect of FOX-7 on thermal decomposition of AP and HMX/AP mixture: The thermal decomposition and combustion behaviour of AP in the presence of HMX, along with the performance optimisation of AP/HMX binary mixtures arising from their mutual interactions during decomposition, have been reported in the literature [3]. Since AP is a major constituent of composite solid propellants, it is essential to investigate its influence on FOX-7/HMX binary mixtures as well as on propellant formulations. Therefore, the present study was undertaken to examine the effect of AP on FOX-7/HMX mixtures and corresponding solid propellant systems.

Neat HMX is thermally stable and decomposes at approximately 285 ºC. However, in binary and ternary mixtures containing AP and FOX-7, the decomposition behaviour of HMX was significantly altered, as shown in Fig. 8. In the FOX-7/AP mixture, the thermal decomposition stages of AP shifted to lower temperatures by nearly 40 ºC. The low-temperature decomposition (LTD) and high-temperature decomposition (HTD) peaks of AP shifted from 285 ºC and 385 ºC to 242 ºC and 340 ºC, respectively. These observations indicate strong mutual interactions between FOX-7 and AP during the thermal decomposition.

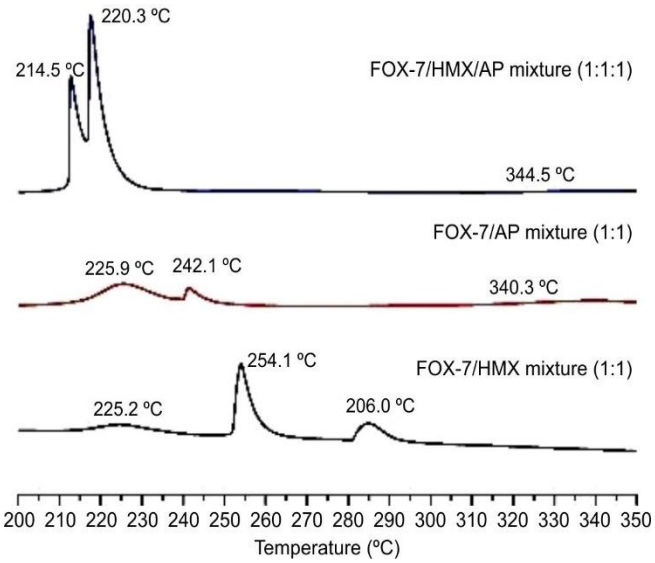

Fig. 8. DSC curves of HMX/FOX-7, FOX-7/AP and FOX-7/HMX/AP mixtures as a function of HMX content

According to the present TG–FTIR analysis, FOX-7 decomposition evolves NO_2 during both decomposition stages, whereas AP decomposition produces NH_3 during the first-stage decomposition [3]. The significant lowering of AP decomposition temperatures in the presence of FOX-7 may therefore be attributed to the catalytic influence of NO_2 on AP decomposition. Similarly, the NH_3-rich environment generated during AP decomposition may have contributed to shifting both decomposition stages of FOX-7 to around 225.9 ºC.

For the ternary HMX/FOX-7/AP mixture, the decomposition events occurred at 214.5 ºC, 220.3 ºC and 344 ºC, corresponding to FOX-7, HMX and AP decomposition, respectively (Fig. 8). The decomposition process was likely initiated by NO_2 and NH_3 released from FOX-7 and AP, which subsequently promoted the decomposition of HMX. The substantial reduction in HMX decomposition temperature from 285.7 ºC to 220.3 ºC confirms the strong influence of NO_2 and NH_3 generated during the decomposition of FOX-7 and AP, respectively [3]. Thus, the thermal decomposition behaviour of the individual energetic components was significantly altered in the ternary HMX/FOX-7/AP system, demonstrating strong mutual interactions among the constituents and resulting in decomposition temperatures markedly different from those of the neat materials.

Physical, thermal decomposition and burning rate behaviour of energetic propellants: Formulation of reduced smoke propellants with optimum ballistic and sensitivity properties is the main objective of the study. Several researchers studied the advantages on the incorporation of FOX-7 in the propellant formulations [32-26]. Xie *et al.* [32] reported that incorporation of FOX-7 improved friction and impact sensitivities by 12% and 38%, respectively. Further, pressure exponent was suppressed by ~5% by replacement of FOX-7 with HMX.

In present study, HMX containing propellants were formulated using energetic binder along with oxidiser AP and FOX-7. Reduced smoke propellants having unary, binary and ternary solids of FOX-7, HMX and AP were formulated to understand the effect of thermal decomposition pattern observed in unary, binary and ternary mixtures of FOX-7, HMX and AP using TG-FTIR. Propellant samples were prepared having formulations P-1, P-2 and P-3 propellants were processed and the formulations are shown in Table-2.

TABLE-2
FORMULATION OF ENERGETIC PROPELLANTS

Ingredient	P-1	P-2	P-3
Energetic binder	26	26	26
AP	–	–	20
HMX	–	30	30
FOX-7	74	44	24

True densities of the energetic propellants were measured using the gas displacement method with a helium pycnometer. Sample volumes were determined under isothermal conditions using ultra-high purity helium and skeletal densities were calculated from the averaged mass-to-volume ratio over multiple measurement cycles. The measured densities of P-1, P-2 and P-3 were 1.63 g/cc, 1.68 g/cc and 1.71 g/cc, respectively. The progressive increase in density from 1.63 to 1.71 g/cc is attributed to the incorporation of high-density HMX and AP, resulting in improved packing efficiency. FOX-7 contributed to reduced sensitivity, while HMX enhanced the energetic performance. The addition of AP further increased the density and reactivity owing to its oxidizing nature. The energetic propellants P-1, P-2 and P-3 followed these trends.

Impact sensitivity increased with the incorporation of HMX and AP. The impact sensitivity decreased from 14.8 J for P-1 to 12.6 J for P-2 after the incorporation of HMX and further decreased to 10.5 J for P-3 with the addition of AP. Thermal behaviour of formulation P-1 containing the energetic binder and FOX-7 was evaluated using DSC, as shown in Fig. 9a. The thermogram exhibited a distinct two-stage exothermic decomposition profile. The initial stage is characterised by a broad exothermic peak centred at 226.1 ºC, primarily attributed to the thermal degradation of the energetic binder components. This is followed by a sharp and intense exothermic peak at 272.0 ºC corresponding to the main decomposition of FOX-7 crystals. The clear separation between these thermal events indicates a stepwise degradation process in which the relatively less stable binder decomposes prior to FOX-7 due to the influence of decomposition products from the energetic binder matrix.

The DSC profile of P-2 propellant is shown in Fig. 9b. The initial stage exhibited a broad, low-intensity exothermic peak centred at 228.1 ºC, corresponding to the preliminary decomposition of the energetic binder matrix. This was followed by a single sharp and highly intense exothermic peak at 251.9 ºC corresponding to the combined decomposition of HMX and FOX-7 crystalline fillers. The merging of HMX and FOX-7 decomposition peaks into a single exothermic event indicates strong thermal interactions within the formulation. This suggests that the initial decomposition products of the binder and energetic fillers catalyse rapid decomposition of the entire formulation.

The thermal decomposition profile of P-3 propellant shown in Fig. 9c revealed a complex two-stage exothermic degradation behaviour dominated by a sharp high-enthalpy exothermic peak at 246.1 ºC. This major thermal event corresponds to the simultaneous decomposition of the energetic matrix and crystalline fillers and exhibits a significant shift towards lower temperature compared to AP-free formulations. This pronounced thermal destabilisation indicates strong interactions in which the oxidative decomposition products of AP catalyse the decomposition of HMX and FOX-7, resulting in rapid energy release. A secondary broad exothermic peak was observed at 297.9 ºC, corresponding to the high-temperature decomposition stage of residual AP and its intermediate decomposition species. Thus, these thermal results confirm that the incorporation of AP acts as a strong thermal sensitiser, lowering the activation barrier and accelerating the decomposition of the heterogeneous energetic matrix.

The burning rates of P-1, P-2 and P-3 propellants were evaluated under nitrogen pressure and are shown in Table-3. The burning rate of P-1 was lower than those of P-2 and P-3 due to FOX-7-based monopropellants exhibit lower burning rates compared to HMX- and AP-containing formulations. The burning rate of P-2 was 7.20 mm/s at 6.9 MPa, which is

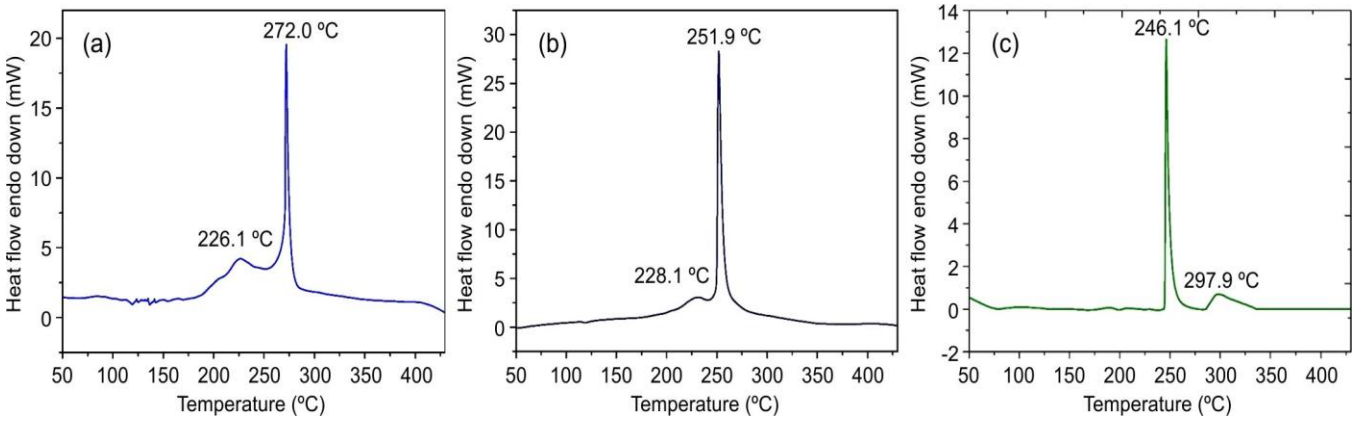

Fig. 9. Comparative decomposition profiles (DSC) recorded at 10 ºC for (a) P-1, (b) P-2 and (c) P-3

TABLE-3
BURNING RATES OF ENERGETIC PROPELLANTS AT VARIOUS PRESSURES

Pressure (kgf/cm^2)	P-1 (Binder/FOX-7) (mm/s)	P-2 (Binder/FOX-7/HMX) (mm/s)	P-3 (Binder/FOX-7/AP/HMX) (mm/s)
70	6.59	7.20	9.08
90	7.83	8.08	10.22
110	9.42	9.43	11.49
130	9.48	10.31	12.82
n (70-130)	0.63	0.59	0.56

approximately 9% higher than P-1 and about 20% lower than P-3. The enhanced burning rate of P-2 compared to P-1 is attributed to the lowering of HMX decomposition temperature by nearly 30 ºC due to the mutual interaction between FOX-7 and HMX, as discussed in Fig. 5. In case of P-3, the energetic components decomposed at significantly lower temperatures than in P-1 and P-2, resulting in higher burning rates.

The pressure exponent of P-1 was 0.63, which decreased to 0.59 and 0.56 for P-2 and P-3, respectively. As pressure increases during combustion, the interaction between the flame zone and burning surface becomes stronger, enhancing heat feedback and increasing burning rates [37]. Catalysed propellants generally exhibit higher burning rates even at lower pressures due to the reduced distance between the flame zone and burning surface [38]. In present study, the mutual interactions among the decomposition products appear to promote combustion and reduce the flame stand-off distance. The extent of this mutual effect increased from P-1 to P-3, leading to improved combustion efficiency and reduced pressure dependency of burning rate. The effect became more pronounced with increasing pressure from 6.9 MPa to 12.75 MPa.

Conclusion

HMX/FOX-7 mixtures with varying mass ratios were successfully prepared using the wet grinding technique without the formation of new crystalline phases indicating that the interaction between the components is predominantly physical in nature. Thermal investigations using TG–DSC–FTIR revealed that the 1:1 HMX/FOX-7 mixture exhibited a distinct multistep decomposition behaviour compared to the individual constituents, confirming strong mutual interactions during thermal degradation. FTIR analysis of evolved gases demonstrated that NO_2 released from FOX-7 plays a significant role in initiating HMX decomposition, leading to characteristic decomposition pathways involving the formation of N_2O and other gaseous species. The relatively higher activation energy of the mixture compared to FOX-7 further indicates improved resistance towards thermal initiation. Therefore, the combination of FOX-7 and HMX significantly modifies both the kinetics and mechanism of thermal decomposition. Energetic propellants based on unary, binary and ternary combinations of FOX-7, HMX, and AP were formulated as P-1, P-2, and P-3, respectively, and evaluated in terms of density, impact sensitivity, thermal stability and burning behaviour. DSC studies revealed a reduction in the decomposition temperatures of the individual energetic components in the presence of other propellant constituents, which may be attributed to solid–solid and gas–solid interactions among the decomposition products during thermal degradation. The mutual interactions became more pronounced in the ternary formulations and under elevated pressure conditions, resulting in enhanced burning rates and reduced pressure dependency. The pressure exponent decreased from 0.63 for P-1 to 0.56 for P-3 over the pressure range of 6.9-12.75 MPa, indicating improved combustion behaviour due to stronger interaction between the flame zone and burning surface.

ACKNOWLEDGEMENTS

The authors are grateful to the Director, High Energy Materials Research Laboratory (HEMRL), Pune, India for constant encouragement and permission for publishing the work.

CONFLICT OF INTEREST

The authors declare that there is no conflict of interests regarding the publication of this article.

DECLARATION OF AI-ASSISTED TECHNOLOGIES

During the preparation of this manuscript, the authors used an AI-assisted tool(s) to improve the language. The authors reviewed and edited the content and take full responsibility for the published work.

REFERENCES

1. Z.-H. Xue, Z.-K. Wang, R.-X. Xu, X.-X. Zhang and Q.-L. Yan, *Energ. Mater. Front.*, **3**, 209 (2022); https://doi.org/10.1016/j.enmf.2022.01.005
2. J. Dong, J. Peng, C. Li, J. Ou, and J. Liu, *Cent. Eur. J. Energ. Mater.*, **22**, 344 (2025); https://doi.org/10.22211/cejem/211476
3. A.N. Pivkina, N.V. Muravyev, K.A. Monogarov, V.G. Ostrovsky, I.V. Fomenkov, Y.M. Milyokhin and N.I. Shishov, in eds.: L. De Luca, T. Shimada, V. Sinditskii and M. Calabro, Synergistic Effect of Ammonium Perchlorate on HMX: From Thermal Analysis to Combustion, In: Chemical Rocket Propulsion, Springer, pp 365-381 (2017); https://doi.org/10.1007/978-3-319-27748-6_15
4. K. Hwang, H. Mun, J.Y. Jung, H.L. Cho, S.J. Kim, B.S. Min, H.B. Jeon and W. Kim, *Polymers*, **11**, 1966 (2019); https://doi.org/10.3390/polym11121966
5. S.M. Pande, V.S. Sadavarte, D. Bhowmik, D.D. Gaikwad, R.V. Singh and H. Singh, *Propellants Explos. Pyrotech.*, **37**, 241 (2012); https://doi.org/10.1002/prep.201000149
6. K. Menke and S. Eisele, *Propellants Explos. Pyrotech.*, **22**, 112 (1997); https://doi.org/10.1002/prep.19970220304
7. C. Oommen and S.R. Jain, *J. Hazard. Mater.*, **67**, 253 (1999); https://doi.org/10.1016/S0304-3894(99)00039-4
8. I. Powell, Reduced Vulnerability Minimum Smoke Propellants For Tactical Rocket Motors, Proceedings of 41st AIAA/ASME/SAE/ASEE Joint Propulsion Conference, AIAA Paper 2005-3615 (2005); https://doi.org/10.2514/6.2005-3615
9. M. Nagamachi, J. Oliveira, A. Kawamoto and R. Dutra, *J. Aerosp. Technol. Manag.*, **1**, 153 (2009); https://doi.org/10.5028/jatm.2009.0102153160
10. K. Menke, T. Heintz, W. Schweikert, T. Keicher and H. Krause, *Propellants Explos. Pyrotech.*, **34**, 218 (2009); https://doi.org/10.1002/prep.200900013
11. N. Wingborg, S. Andreasson, J. de Flon, M. Johnsson, M. Liljedahl, C. Oscarsson, Å. Pettersson and M. Wanhatalo, Development of ADN-Based Minimum Smoke Propellants, Proceeding of 46th AIAA/ASME/SAE/ASEE Joint Propulsion Conference, AIAA Paper 2010-6586 (2010); https://doi.org/10.2514/6.2010-6586
12. C. Grigore and D.M. Alexandru, *INCAS Bull.*, **9**, 17 (2017); https://doi.org/10.13111/2066-8201.2017.9.1.2
13. I.J. Lochert, DSTO-TR-1238, Defence Science and Technology Organisation (2001).
14. V.P. Sinditskii, A.I. Levshenkov, V.Y. Egorshev and V.V. Serushkin, Proceeedings of 30th International Pyrotechnic Seminar, France, p. 299 (2003).
15. A.K. Burnham, R.K. Weese, R. Wang, Q.S.M. Kwok and D.E.G. Jones, Thermal Properties of FOX-7, Proceedings of 36th International Annual Conference of ICT & 32nd International Pyrotechnics Seminar, Karlsruhe, Germany, 28 June-1 July (2005).
16. R.S. Booth and L.J. Butler, *J. Chem. Phys.*, **141**, 134315 (2014); https://doi.org/10.1063/1.4896165
17. W.A. Trzciński and A. Belaada, *Cent. Eur. J. Energ. Mater.*, **13**, 527 (2016); https://doi.org/10.22211/cejem/65000
18. M. Ghosh, A.K. Sikder, S. Banerjee, M.B. Talawar and N. Sikder, *Def. Technol.*, **16**, 188 (2020); https://doi.org/10.1016/j.dt.2019.05.018
19. P.B. Kempa, M. Hermann, F.J.M. Metzger, V. Thome, A. Kjellstroem and N. Latypov, Proceedings of 35th International Annual Conference ICT, pp. 71/1-71/5 (2004).
20. R. Wild and U. Teipel, Proceedings of 35th International Annual Conference ICT, p. 69/1-69/9 (2004).
21. J. Welch, Ph.D. Thesis, Low Sensitivity Energetic Materials Ludwig Maximilian University of Munich (2008).
22. M.J. Crawford, J. Evers, M. Göbel, T.M. Klapötke, G. Oehlinger, P. Mayer and J.M. Welch, *Propellants Explos. Pyrotech.*, **32**, 478 (2007); https://doi.org/10.1002/prep.200700240
23. D.S. Viswanath, T.K. Ghosh and V.M. Boddu, FOX-7 (1,1-Diamino-2,2-Dinitroethylene), In: Emerging Energetic Materials: Synthesis, Physicochemical and Detonation Properties. Springer (2018); https://doi.org/10.1007/978-94-024-1201-7_3
24. O. Ordzhonikidze, A. Pivkina, Y. Frolov, N. Muravyev and K. Monogarov, *J. Therm. Anal. Calorim.*, **105**, 529 (2011); https://doi.org/10.1007/s10973-011-1562-1
25. S. Vyazovkin, *Molecules*, **25**, 2813 (2020); https://doi.org/10.3390/molecules25122813
26. A. Kumar, V.S. Sadavarte, S.S.N.M. Santosh Mada, S.M. Pande and P.V. Chavan, *Propellants Explos. Pyrotech.*, **46**, 626 (2021); https://doi.org/10.1002/prep.202000241
27. N. Koga, S. Vyazovkin, A.K. Burnham, L. Favergeon, N.V. Muravyev, L.A. Perez-Maqueda, C. Saggese and P.E. Sanchez-Jiménez, *Thermochim. Acta*, **719**, 179384 (2023); https://doi.org/10.1016/j.tca.2022.179384
28. J. Yu, H. Jiang, S. Xu, H. Li, Y. Wang, E. Yao, Q. Pei, M. Li, Y. Zhang and F. Zhao, *Crystals*, **13**, 167 (2023); https://doi.org/10.3390/cryst13020167
29. X.Y. Liu, X.C. Wang, Y.G. Huang, M.X. Zheng, L. Wang, Y. Jiang and Y.W. Luo, *Guangpuxue Yu Guangpu Fenxi*, **26**, 251 (2006).
30. Y. Xu, R. Chen, Y. Liu, Y. Wang and W. Zheng, *J. Anal. Appl. Pyrol.*, **195**, 107701 (2026); https://doi.org/10.1016/j.jaap.2026.107701
31. T.B. Brill, *J. Propuls. Power*, **11**, 740 (1995); https://doi.org/10.2514/3.23899
32. Z. Fengqi, G. Hongxu, X. Siyu, Y. Jianhua, P. Qing, H. Haixia and X. Xiaoling, *Chin. J. Explos. Propellants*, **33(4)**, 1 (2010) (In Chinese).
33. C. Zhong'e, L. Zhongyou, Y. Nan, L. Qing and W. Du, *Chin. J. Energ. Mater.*, **18**, 316 (2010) (In Chinese); https://doi.org/10.3969/j.issn.1006-9941.2010.03.017
34. D.B. Lempert, E.M. Dorofeenko and Y. Shu, *Russ. J. Phys. Chem. B. Focus Phys.*, **10**, 483 (2016); https://doi.org/10.1134/S1990793116030258
35. T.L. Jensen, E. Unneberg and T.E. Kristensen, *Propellants Explos. Pyrotech.*, **42**, 381 (2017); https://doi.org/10.1002/prep.201600278
36. W. Xie, Y. Zhao, W. Zhang, Y. Liu, X. Fan, B. Wang, W. He and Q.-L. Yan, *Propellants Explos. Pyrotech.*, **43**, 308 (2018); https://doi.org/10.1002/prep.201700251
37. M.W. Beckstead, *Combust. Explos. Shock Waves*, **42**, 641 (2006); https://doi.org/10.1007/s10573-006-0096-5
38. S. Isert and S.F. Son, in eds.: M. Shukla, V. Boddu, J. Steevens, R. Damavarapu and J. Leszczynski, Energetic Materials, Springer, vol. 25 (2017); https://doi.org/10.1007/978-3-319-59208-4_6